Crystal Structures of Rat Thymidylate Synthase Inhibited by Tomudex, a Potent Anticancer Drug[†,‡]

Rogerio R. Sotelo-Mundo,[§] Joanna Ciesla,[||] Jolanta M. Dzik,[||] Wojciech Rode,[||] Frank Maley,[⊥] Gladys F. Maley,[⊥] Larry W. Hardy,[#] and William R. Montfort*[,§]

Department of Biochemistry, University of Arizona, Tucson, Arizona 85721, Nencki Institute of Experimental Biology, Polish Academy of Sciences, 3 Pasteur Street, 02-093 Warszawa, Poland, Wadsworth Center, New York State Department of Health, Albany, New York, 12201, and Department of Pharmacology and Molecular Genetics, University of Massachusetts Medical Center, 55 Lake Avenue North, Worcester, Massachusetts, 01655

Received August 5, 1998; Revised Manuscript Received November 11, 1998

ABSTRACT: Two crystal structures of rat thymidylate synthase (TS) complexed with dUMP and the anticancer drug Tomudex (ZD1694) have been determined to resolutions of 3.3 and 2.6 Å. Tomudex is one of several new antifolates targeted to TS and the first to be approved for clinical use. The structures represent the first views of any mammalian TS bound to ligands and suggest that the rat protein undergoes a ligand-induced conformational change similar to that of the *Escherichia coli* protein. Surprisingly, Tomudex does not induce the "closed" conformation in rat TS that is seen on binding to *E. coli* TS, resulting in inhibitor atoms that differ in position by more than 1.5 Å. Several species-specific differences in sequence may be the reason for this. Phe 74 shifts to a new position in the rat complex and is in van der Waals contact with the inhibitor, while in the *E. coli* protein the equivalent amino acid (His 51) hydrogen bonds to the glutamate portion of the inhibitor. Amino acids Arg 101, Asn 106, and Met 305 make no contacts with the inhibitor in the open conformation, unlike the equivalent residues in the *E. coli* protein (Thr 78, Trp 83, and Val 262). dUMP binding is similar in both proteins, except that there is no covalent adduct to the active site cysteine (Cys 189) in the rat structures. Two insertions in the rat protein are clearly seen, but the N-termini (residues 1−20) and C-termini (residues 301−307) are disordered in both crystal forms.

Thymidylate synthase (TS[1]) catalyzes the reductive methylation of dUMP and is the sole de novo source of dTMP in all species so far examined. The enzyme is of mechanistic interest for the ease with which it catalyzes methyl transfer, of structural interest for its ligand-induced conformational changes, of medicinal interest as a logical target for drug design, and of biological interest for its role in cellular regulation. Several extensive reviews of TS have recently appeared (*1*−*4*).

The majority of the structural and biochemical studies of TS, which began more than 40 years ago (*5*), have been performed with protein isolated from bacterial sources. Since the protein is highly conserved, such studies have enabled the development of potent inhibitors of human TS (hTS), some of which have entered the clinic as anticancer drugs. However, an understanding of several mammalian-specific TS functions has been hampered by the paucity of structural data for these proteins. For example, mammalian TSs appear to have a protein translation regulatory function implemented through binding to its own and other messenger RNA molecules (*6*) and, furthermore, may be regulated through phosphorylation and compartmentalization (between the cytosol and nucleus) (*7*). Once in the nucleus, mammalian TS may be a component of a larger "replisome" (*8*). There is also a growing effort to design drug-resistant forms of hTS that can be used to transfect stem cells of cancer patients, who may then be able to tolerate higher doses of anticancer drugs during treatment (*9*, *10*). Finally, it is of interest to determine the interactions of TS-directed anticancer drugs bound to the drug target, so that any differences between inhibition of mammalian and bacterial TSs can be uncovered.

Nearly all TS inhibitors are analogues of either the TS substrate or the cofactor. The inhibitors discussed in this manuscript, and key aspects of the TS catalytic mechanism, are shown in Figure 1. The reaction catalyzed by TS is the conversion of dUMP to dTMP with the transferred methyl group provided by a cofactor, methylenetetrahydrofolate (CH_2THF). The reaction is initiated through nucleophilic

[†] This work was supported by NIH Grant HL54826 (W.R.M.); ACS Grant RPG-93-041-04-CDD (W.R.M.); ADCRC Grant 1-208A (W.R.M.); NCI Grant CA44355 (F.M.), NSF Grant MCB-9724071 (G.F.M.), the State Committee for Scientific Research Grant No. 4 P05F 030 11p02 (W.R.), the Council on Tobacco Research (L.W.), and the AHA (L.W.). R.R.S. is supported by a predoctoral fellowship from CONACYT Mexico and CIAD.

[‡] Coordinates have been deposited in the Brookhaven Protein Data Bank for both rTS ternary complexes (accession numbers 1rts and 2tsr).

* Corresponding Author. E-mail: montfort@u.arizona.edu.

[§] University of Arizona.

[||] Nencki Institute of Experimental Biology.

[⊥] Wadsworth Center.

[#] University of Massachusetts Medical Center. Current address: ArQule Inc., 303 Bear Hill Road, Waltham, MA 02154.

[1] Abbreviations: TS, thymidylate synthase; rTS, recombinant rat hepatoma TS; rhTS, TS from rat hepatoma cells; rrlTS, TS from regenerating rat liver; hTS, human TS; ecTS, *Escherichia coli* TS; lcTS, *Lactobacillus casei* TS; methylenetetrahydrofolate, CH_2THF.

10.1021/bi981881d CCC: $18.00
Published on Web 12/29/1998

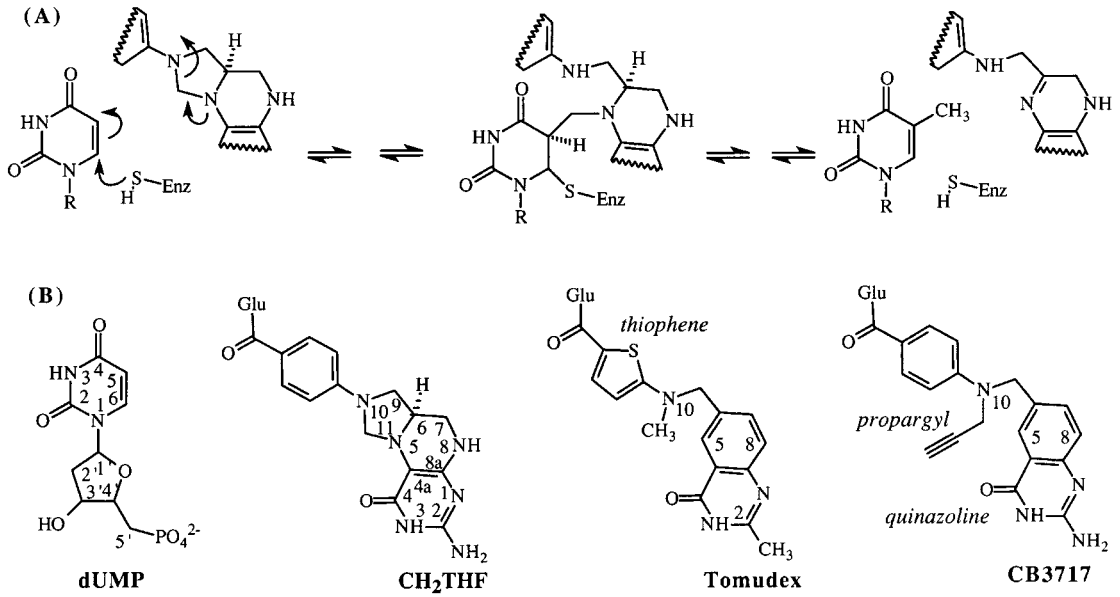

FIGURE 1: TS catalytic mechanism and inhibitor structure. (A) Simplified mechanism. (B) Structures of substrate dUMP, cofactor *6R* 5,10-methylenetetrahydrofolate (CH_2THF), and inhibitors Tomudex (ZD1694) and CB3717.

attack of the dUMP pyrimidine by an active site thiol, and by opening of the CH_2THF five-membered ring. An intermediate is formed that contains covalent bonds between the substrate and both the protein and the cofactor, which is followed by formation and release of the products, dTMP and dihydrofolate. The enzyme undergoes an extensive conformational change during catalysis that results in burial of the ligands in the active site and modulates the chemistry of the thiol adduct (*11*−*13*). Recent detailed discussions of the TS mechanism can be found in refs *11*, *14*, and *15*.

Analogues of both substrate and cofactor have proven to be excellent inhibitors of TS, and two such compounds have reached clinical use for the treatment of cancer. 5-Fluorouracil, which is metabolically converted to 5-fluoro-dUMP (FdUMP), has been used in the treatment of breast and colon cancer for over 40 years, with moderate success. Tomudex (ZD1694, shown in Figure 1) is one of several new folyl-based TS inhibitors developed for cancer treatment, and is the only TS-directed antifolate so far approved for cancer treatment (in Europe). Tomudex, like most of the other new antifolates, is derived from an earlier inhibitor (CB3717, Figure 1) that failed in the clinic for reasons related to solubility (reviewed in refs *16*, *17*).

Ideally, structures of hTS in the presence and absence of substrates and inhibitors should be determined. However, structural studies of hTS have been compromised by the poor quality of hTS crystals, and the only reported hTS structure is at low resolution and in the absence of ligands (*18*). We have therefore pursued the structure of the rat protein, which is 90% identical to the human protein overall, and completely identical in the active site.

In the present work, we present two structures of rat TS (rTS) complexed with dUMP and Tomudex, one to 3.3 Å nominal resolution and the other to 2.6 Å nominal resolution. In both structures, ligands are bound in an arrangement similar to that in the identical complex with *Escherichia coli* TS (ecTS) (*19*), except that the inhibitor has failed to induce a closed protein conformation in rTS and failed to stabilize the thiol adduct with dUMP. Thus, these complexes not only present the first inhibitory structures of a mammalian TS, but also suggest an unexpected difference in the binding of Tomudex to the bacterial and mammalian TSs.

MATERIALS AND METHODS

Protein Isolation, Characterization, and Inhibition. Recombinant rat hepatoma TS (rTS) was prepared from an overexpressing *E. coli* strain as previously described (*20*), except that a second DEAE-cellulose chromatography column was added. The recombinant protein was judged to be near homogeneity by denaturing polyacrylamide slab gel electrophoresis using a 20 μg sample (*21*), and to be fully active. Enzyme activity was measured spectrophotometrically (*22*), and the specific activity was found to be 2.4 μmol min^{-1} mg^{-1} for conversion of dUMP to dTMP at 30 °C. The protein's N-terminus was sequenced (University of Arizona Laboratory for Protein Sequencing and Analyses) and found to be fully intact. The mass of the protein was measured from two different protein batches and found to be 35 009 Da for the first sample and 35 012 Da for the second. Both values are within experimental error of the predicted mass for the intact protein (35 015 Da). Rat TSs from hepatoma cells (rhTS) and from regenerating rat liver (rrlTS) were purified as previously described (*23*, *24*). These proteins displayed a specific activity about 4-fold less than that of the recombinant protein (*23*, *24*), possibly due in part to a modification of the N-terminus in rat cells, as previously discussed (*20*). The rTS, rhTS, and rrlTS proteins were indistinguishable by SDS−PAGE.

Quantitative analyses of TS reaction kinetics and inhibition were performed using an assay that measures tritium release from [5-^{3}H]dUMP, as previously described (*25*). Inhibition by Tomudex was evaluated with an algorithm employing nonlinear regression analysis for competitive, noncompetitive, and mixed inhibition types (*25*).

Crystallization and Data Collection. Recombinant rTS was prepared from an ammonium sulfate precipitate. Two crystal forms were obtained, both in space group *C*2. For crystal

form 1, the protein was diluted into a buffer of 50 mM TES (pH 7.4), 5 mM DTT, and exchanged several times using a Centricon-10, resulting in a final protein concentration of 35 mg/mL. dUMP and Tomudex (a gift from Dr. Tom Boyle, Zeneca Pharmaceuticals) were added to a final concentration of 2.3 mM, and crystals were obtained by the hanging drop method at 4 °C after mixing 1:1 with a well buffer solution of 21% (weight/volume) PEG 4000 (Fluka), 0.1 M Tris HCl buffer (pH 8.5), and 0.2 M magnesium chloride. Data were measured from a single flash-frozen crystal (−170 °C in original buffer) measuring 0.25 × 0.1 × 0.1 mm (a = 159.6 Å, b = 88.5 Å, c = 68.8 Å, β = 97.8°), using a MAR imaging plate and Cu Kα radiation. Data were processed with Denzo and Scalepack (*26*).

Crystal form 2 was obtained at room temperature by the hanging drop method from protein dialyzed against a buffer containing 5 mM DTT and 20 mM TES, pH 7.4. A solution of protein (32 mg/mL), dUMP (6 mM), and Tomudex (6 mM) was mixed 1:1 with a well buffer of 20% (weight/volume) PEG 5000 monomethyl ether, 200 mM ammonium sulfate, 5 mM DTT, and 100 mM MES, pH 6.0. Crystals of approximately 0.7 × 0.5 × 0.2 mm were obtained (a = 99.7 Å, b = 101.6 Å, c = 140.8 Å, β = 101.4°). Data were measured from two crystals using an Enraf Nonius area detector and Cu X-ray source and were processed with MADNES (*27*), PROCOR (*28*), and CCP4 (*29*).

Structure Determinations. The structure of crystal form 1 was determined by molecular replacement using an *E. coli* TS ternary complex (*12*) as a starting model, with ligands and solvent molecules removed, and the program X-PLOR (*30*, *31*). The crystals contained one TS dimer in the asymmetric unit (Matthew's coefficient = 3.57) (*32*)). The rotation function contained 2-fold related peaks corresponding to the two monomers in the dimer, and rigid body refinement of the translation search result yielded an initial model with R_{crys} = 0.45 and clear electron density for the ligands. The final model was obtained after rounds of model building with O (*33*) and refinement with X-PLOR (*34*, *35*). Two overall temperature factors were refined for each residue, one each for the main chain and side chain atoms, and noncrystallographic symmetry restraints were applied throughout refinement.

The structure of crystal form 2, which contains two TS dimers in the asymmetric unit (Matthew's coefficient = 2.59), was determined by molecular replacement using the rTS model from crystal form 1, except that ligands and residues 20−30 were removed. A low-resolution model was obtained using data from a crystal that diffracted to 3.5 Å by first placing one dimer in the orientation indicated by the highest peak in the cross-rotation function, followed by a translation search (R_{crys} = 0.44), and then placing the second dimer based on the highest peak in the self-rotation function, followed by a translation search in the absence of the first dimer. After rigid body refinement of both dimers, R_{crys} dropped to 0.33. Clear electron density was observed for omitted residues 20−30 in the initial difference electron density maps, but electron density was absent for the ligands until the structure was better refined. The final model was refined against data from a second crystal that was slightly nonisomorphous with the first crystal, but which extended to 2.6 Å resolution (Table 1). Noncrystallographic symmetry was initially restrained during refinement but was eventually left unrestrained, and individual isotropic temperature factors were refined for each atom.

Table 1. Data Collection and Refinement Parameters

	crystal form 1	crystal form 2 (a)	crystal form 2 (b)
space group	*C*2	*C*2	*C*2
a (Å)	159.6	100.0	99.7
b (Å)	88.5	101.8	101.6
c (Å)	68.8	141.2	140.8
β (deg)	97.8	101.3	101.4
resolution (Å)	15−3.3	20−3.5	8−2.6
unique reflections	14 261	17 106	35 484
multiplicity	5.58	2.5	1.8
completeness (%)[a]	100/100	97/97	85/71
$I/\sigma(I)$	18/11.3	5.4/3.2	10.3/2.6
R_{sym}[b]	8/14.2	11.9/21.8	5.6/21.4
R_{crys}[c] (working set/test set)	0.19/0.23		0.16/0.22
rmsd, ideal distances (Å)	0.008		0.008
rmsd, ideal bond angles (deg)	1.3		1.4
most favored phi/psi (%)	90		90
$\langle B \rangle$, protein atoms (Å^2)	27		39
$\langle B \rangle$, ligand atoms (Å^2)	35		68
no. solvent molecules	0		75

[a] Total/outer shell. [b] $R_{sym} = (\sum_h |I_h - \langle I \rangle|)/(\sum_h I_h)$. [c] $R_{crys} = (\sum_h |F_{obs} - F_{calc}|)/(\sum_h F_{obs})$, where the working and test sets are as implemented in X−PLOR (*47*).

Structure comparisons were performed with INSIGHTII (Biosym Technologies, San Diego), and figures were drawn with O (*33*), MOLSCRIPT (*36*), BOBSCRIPT (*37*).

RESULTS

Inhibition of rTS by Tomudex. The recombinant protein was purified to near homogeneity and displayed the expected specific activity (see methods for details). The inhibition of rTS by Tomudex was competitive with respect to CH_2THF, and similar in magnitude to that reported for human and murine TSs. The recombinant protein displayed K_i = 29 ± 8 nM (mean ± standard error for three measurements), whereas K_i = 62 nM for murine TS and apparently ∼60 nM for hTS (*16*). The mode of inhibition was reported to be slightly mixed noncompetitive for inhibition of the mouse protein (*38*). Inhibition of rat TS isolated from regenerating rat liver (rrlTS) has also been reported and found to display competitive inhibition with K_i = 100 nM (*25*). For ecTS, K_i = 1 μM, 10−34-fold higher than for rTS and hTS (L. Hardy, unpublished data).

Structure of rTS-dUMP-Tomudex (Crystal Form 1). The first crystal form obtained for the rTS-dUMP-Tomudex contained one TS dimer in the asymmetric unit and yielded diffraction data to 3.3 Å resolution. The structure was determined by molecular replacement (see Methods for details). Despite the low resolution, the ligands were well-ordered in the active site and displayed readily discernible conformations in the final electron density map (Figure 2).

Surprisingly, the protein was in the open conformation, where the covalent adduct between substrate and the active site cysteine (Cys r189) cannot form.[2] This is in contrast to the complex formed with ecTS, where the covalent adduct to dUMP was found (*19*), and further, in contrast to all ecTS

[2] Numbering: The residue number used is for the species indicated, where "r" refers to rat, "h" to human, etc. For example, Cys r189 is cysteine 189 for the rat protein.

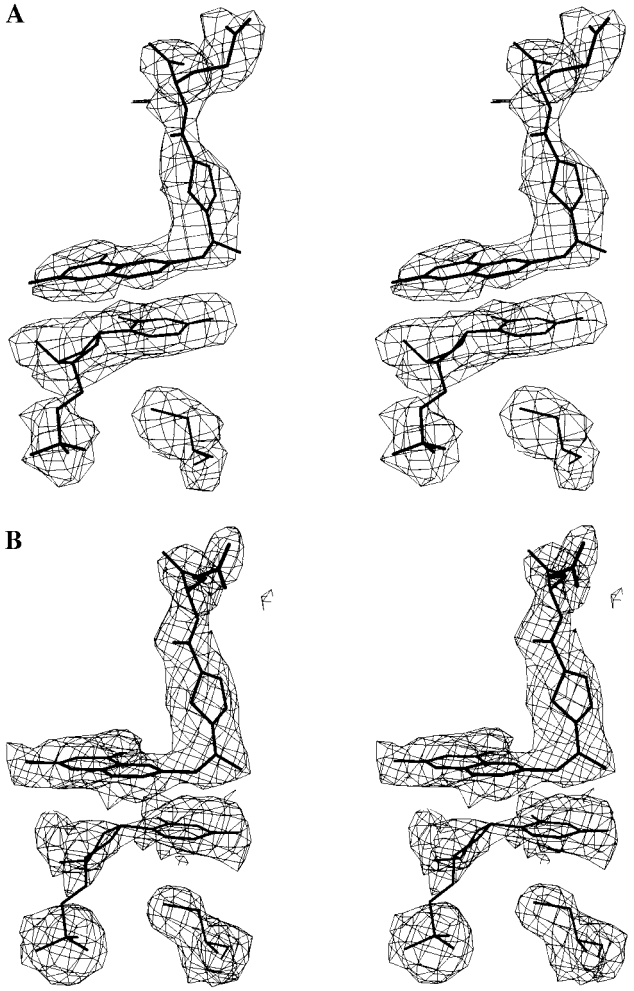

FIGURE 2: Simulated annealed "omit" electron density maps for ligands. Ligands and Cys r189 were removed from the model followed by simulated annealing to remove phase bias (*46*) and maps calculated using $(F_o - F_c)\alpha_c$ coefficients (contour level = 2σ): (A) crystal form 1, monomer A; (B) crystal form 2, monomer C.

ternary complexes determined to date, which are all in the closed conformation (reviewed in ref *1*).

Both the N- and C-termini were disordered in the first rTS structure, and residues r1−r20 and r301−r307 were therefore left out of the final model. The rat N-terminus is 23 amino acids longer than ecTS; however, only three of the additional residues were found in the structure (r21−r23). Replacing the *E. coli* N-terminal methionine is Glu r24, which forms hydrogen bonds to Thr r69 and Thr r70 in an arrangement similar to that found in lcTS (*39*). In ecTS, the N-terminus forms a carbamate with CO_2 in order to retain these hydrogen bonds (*40*). There are two additional insertions in rTS with respect to ecTS (r111−r122, and r140−r147), and although these loops were more poorly ordered than the rest of the protein, the general fold for these insertions was apparent (Figure 3).

Ligand binding in the rTS complex is very similar to that observed for the ecTS-dUMP-Tomudex structure (*19*), except that the more open protein conformation leads to fewer protein−ligand contacts (discussed below).

Structure of rTS-dUMP-Tomudex (Crystal Form 2). A second crystal form was found that diffracted to higher resolution and contained two full TS dimers (~140 kDa) in the asymmetric unit, resulting in a 2.6 Å structure of the rTS ternary complex (see Methods for details). The four monomers in crystal form 2 are nearly identical to each other and to the model of crystal form 1. The protein in crystal form 2 is once again in the open conformation (slightly more so than crystal form 1), and the N- and C-termini are once again disordered. The loop containing Arg r44, which contacts both the dUMP phosphate and the C-terminus in the ecTS closed conformation, is very poorly ordered in crystal form 2, and its position in the model is unreliable. The rTS insertions are better defined in crystal form 2, although they are still less well ordered than some other portions of the protein, and they display the same conformations as in crystal form 1. The ligands are present in all active sites, but are more poorly ordered than in the first crystal form (Figure 2). The electron density for monomers C and D is better than for monomers A and B in the crystal.

The final models for the four monomers in the second crystal form consist of the same residues as the two monomers in crystal form one: amino acids r21−r300. Residues r1−r20, and r301−r307 are not visible in any of the six independent monomers resulting from the two crystal structure determinations. That these amino acids were present in the protein was confirmed by mass spectrometry, N-terminal sequencing, and gel electrophoresis, as noted above.

Ligand Binding in rTS-dUMP-Tomudex. The ligand arrangements in the ecTS and rTS ternary complexes are quite similar except that contacts to the "right" side of the rat active site (as displayed in Figure 3) are fewer in number, and contacts to the C-terminus are completely missing. All contacts with dUMP found in the ecTS complex were found in rTS except for the covalent adduct with Cys r189, which cannot form when the protein is in the open conformation (illustrated in Figure 4A). The Cys r189 sulfur and the pyrimidine ring are in van der Waals contact (3.5 Å in monomer C of crystal form 2),[3] but the residue is poorly aligned for nucleophilic attack, and the ligand is unable to shift the ~1.5 Å required for covalent addition without either a shift of the protein to the closed conformation or a loss of several hydrogen bonds to the pyrimidine ring (Arendall and Montfort, unpublished data, and discussed in ref *1*). All nine residues that hydrogen bond to dUMP in ecTS (*12, 41*) also hydrogen bond in rTS, except for Arg r44, which is poorly ordered as noted above. However, several of the ordered water molecules found in the ecTS ternary complexes, including the water linking O4 of the pyrimidine and the carboxylate of Glu ec58, were absent in the rat structure. This is probably a consequence of the open conformation, which provides more room for solvent in the active site, allowing for greater solvent disorder.

In contrast to dUMP binding, there were several differences in the way Tomudex binds to rTS and ecTS (Figure 4). The first differences are due to the open conformation found in rTS. van der Waals contacts between Tomudex and Ile r102, Trp r103, Leu r215, Gly r216, and Phe r219 in the rat complex are similar to those found in *E. coli* complex, although Phe r219 rotates to a new position (see below). The expected hydrogen bond between the side chain of Asp r212 and Tomudex is also present (3.2 Å), but the expected water-

[3] All distances reported are for monomer C of crystal form 2 unless otherwise noted.

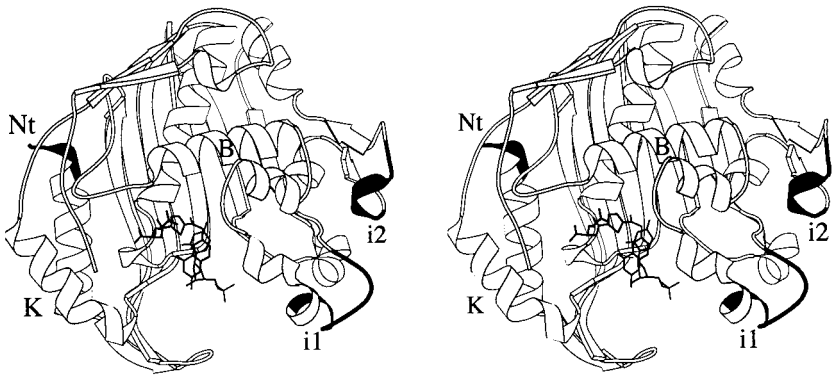

FIGURE 3: Ribbon diagram of rTS-dUMP-Tomudex (stereoview). Shown is one monomer of the rTS dimer. The rTS insertions, with respect to ecTS, are shown in black, as are the ligands. The B and K helices, inserts 1 and 2, and the N-terminus are labeled. Residues r1−r20 and r301−r307 are missing in the model.

mediated hydrogen bond to the C-terminal loop is completely missing, since the loop is disordered, although the water molecule is present in the structure (3.2 Å). Tomudex and dUMP display an extensive van der Waals contact surface in both structures, but the two ligands differ in position by 1−1.5 Å in the two structures (Figure 4C). This difference in position may serve to further dislodge the C-terminus in the rat complex, since the 2-methyl portion of the Tomudex quinazoline overlaps with the expected position for r305 of the C-terminal loop (r301−r307).

Binding may be further altered by two active site differences between the rat and *E. coli* proteins. The first is the change of Trp ec83 to Asn r106. The tryptophan at this position forms van der Waals contacts with the quinazoline ring of Tomudex in the ecTS structure, but the asparagine found in the rat protein cannot form these contacts, the loss of which may contribute to the inability of the inhibitor to induce the closed conformation (Figure 4). The second change is His ec51 to Phe r74 at the "top" of the active site. In the *E. coli* protein, His ec51 points out of the active site. In the rat protein, the loop providing this residue (preceding the B-helix, Figure 3) moves further into the active site, and Phe r74 rotates such that it forms an extensive van der Waals contact with the inhibitor (Figure 4B), and also contacts Phe r219, which shifts further into the active site than does the equivalent residue in ecTS. In this new position, Phe r219 retains extensive van der Waals contacts with the thiophene ring, as noted above, but now contacts Glu r81 on the other side of the active site. For the protein to adopt the closed conformation, Phe r219 would have to move back to a position similar to that found in ecTS, and Phe r74 would likely have to move out of contact with the inhibitor. It should also be noted that in two of the active sites (monomers A and C of crystal form 2), Arg r72 is in contact with the glutamate portion of the inhibitor, but the position of this residue appears to be distorted through crystal packing forces.

A final point worth mentioning is that Tomudex has a 2-methyl group in place of the 2-amino group in CB3717 and CH_2THF (Figure 1). This results in the loss of a hydrogen bond to the C-terminal loop in Tomudex complexes, which may lead to the open conformation in the rat ternary complex, where binding is already compromised from changes to residues r74 and r106, but still permit formation of the closed conformation in the ecTS complex.

Comparison of rTS with the Bacterial Homologues. TS is perhaps the most highly conserved enzyme known, with the bacterial and mammalian TSs having ∼50% sequence identity. It is therefore not surprising that the structures of the bacterial and rat TSs are also nearly identical. The ligand binding arrangement for ligands is nearly identical in rTS and ecTS, as discussed above, and the N-terminal hydrogen bonding to Thr r69 and Thr r70 is conserved. Two insertions (r111−r122, and r140−r147) form extensions of shorter loops found in ecTS and have essentially no effect on either the local fold at the point of insertion or the general TS fold. Insertions after residue r111 occur in both rTS and lcTS, but interestingly, the rTS insertion looks nothing like that of lcTS (*42*), suggesting either that the insertion does not have a functional role in TS or that the functional role is species-specific. The second rTS insertion (after residue r140) leads to an alternate conformation for the loop containing the insertion. The residues in this insertion are conserved in mammalian TSs and may play a functional role in higher species, such as providing a surface for binding to other cellular proteins. The conformation of the second insertion is anchored by hydrogen bonds between Tyr r140 and Thr r90 and between Tyr r147 and Asp r142.

The most surprising difference found in the present structures is that the protein conformation of rTS-dUMP-Tomudex is open, while that of ecTS-dUMP-Tomudex is closed. The ligand-induced conformational change in TS had been previously characterized only in ecTS, where it was shown to involve the inward shifting of helices and loops on both sides of the active site (*11*−*13*). The largest shift was in the C-terminal loop, which moves 5−6 Å on forming a ternary complex. Additional inward shifts of 0.3−1 Å occur for about half of the remaining amino acids, resulting in an active site volume reduced by nearly 50% (Roberts and Montfort, unpublished data). Superpositioning of the rat ternary complex (monomer C of the second crystal form) with the first monomer of the ecTS-dUMP-Tomudex ternary complex yielded an rms deviation in Cα positions of 2.1 Å, a value greater in magnitude than that for most of the atoms involved in the ligand-induced conformational change. Similar values are obtained for superpositioning with an ecTS-dUMP binary complex (rmsd = 2.0 Å, Roberts and Montfort, unpublished data) and with an lcTS-phosphate binary complex (rmsd = 1.9 Å, (*43*)). Despite this complication, it is clear that the same amino acids that shift on ligand

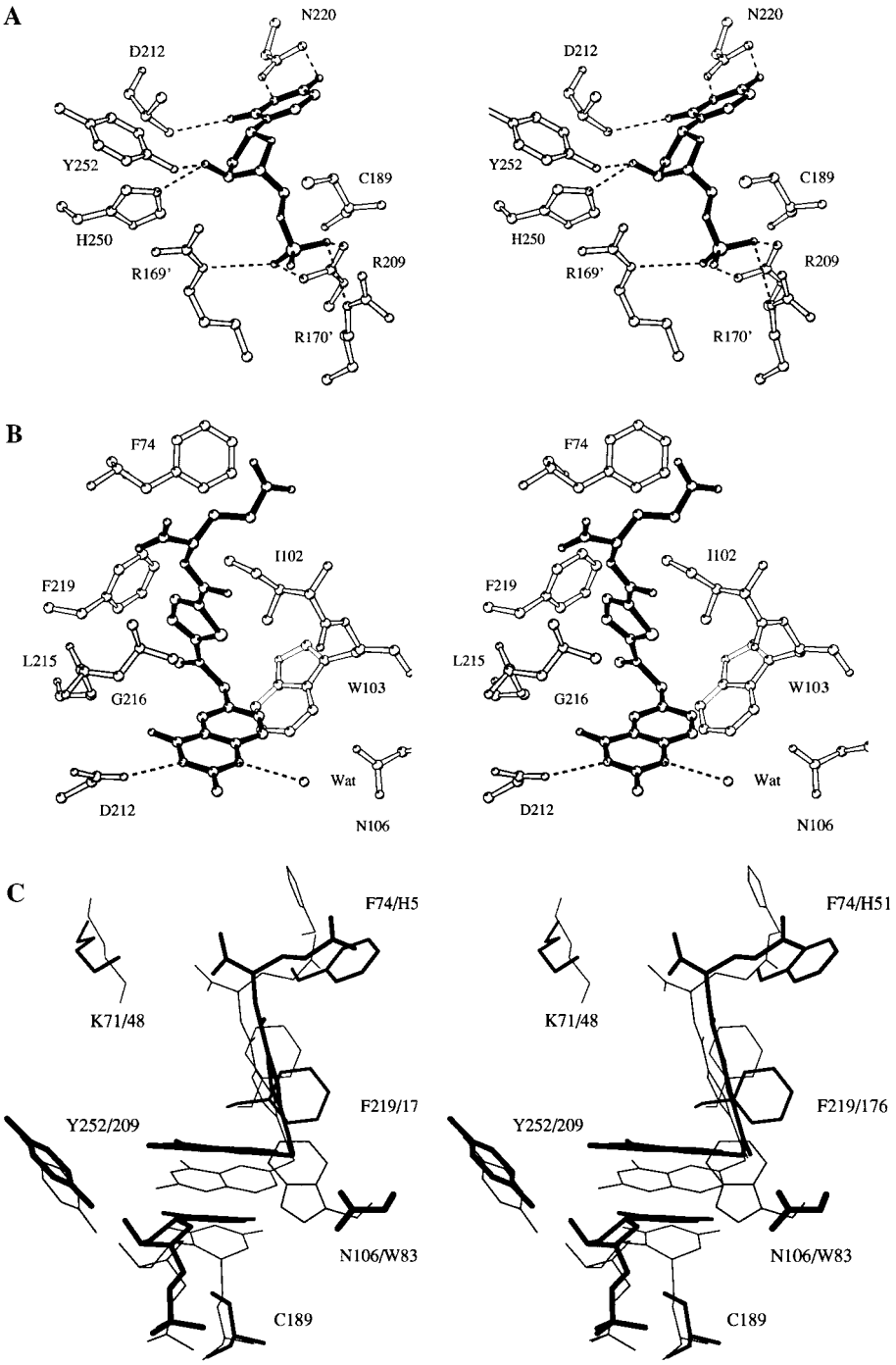

FIGURE 4: Stereoview of ligand binding. (A) dUMP binding in crystal form 1, monomer A (filled bonds). Ser r210 is left out for clarity. Arg r169′ and Arg r170′ are from monomer B. (B) Tomudex binding in crystal form 2, monomer C (filled bonds). (C) Superpositioning of rTS-dUMP-Tomudex (thick lines) and ecTS-dUMP-Tomudex (thin lines).

binding to ecTS also shift in the rTS ternary complex when compared with the ecTS ternary complex. For example, the C-terminus is completely disordered in the rTS structure, and residues on both sides of the active site shift outward by ~1 Å (after superpositioning of the two structures), including the K-helix and preceding residues (r252−r265), and the loop containing Tomudex contact residues Ile r102 and Trp r103. Another indication is that the distance across the active site is about 1 Å further in the rTS structure than in the ecTS ternary complex structure, but is about the same as that for the ecTS and lcTS binary complex structures. For example, the distance between the Cαs for residues Tyr r252 and Cys r189, which contact dUMP from opposite sides of the active site (Figure 4A), is 16.5, 16.4, and 16.2 Å for the "open" complexes rTS-dUMP-Tomudex, ecTS-dUMP, and lcTS-phosphate, but is only 15.4 Å for the "closed" complex ecTS-dUMP-Tomudex.

One difference in the structure determinations of rTS and ecTS is that rTS was crystallized in a solution of moderate ionic strength (0.2 M salt, 20% PEG), while all of the ecTS structures have been crystallized in solutions of >2 M salt. Evidence that this difference in ionic strength is not the reason for the difference in the rTS and ecTS structures comes from the crystal structure of TS from *Leishmania major*, which is a bifunctional enzyme containing both TS and DHFR activities in a single polypeptide (*44*). This protein

was crystallized in 0.12 M ammonium sulfate and 19% PEG in a ternary complex with FdUMP and CB3717, and displayed a closed conformation nearly identical to that of the high-salt ecTS-FdUMP-CB3717 structure (*44*). Interestingly, the *Leishmania* protein also has an Asn substituted for Trp at position r106, as described above for rTS, yet the tighter-binding CB3717 induces the closed conformation in this protein despite the loss of contacts with this residue.

Comparison of hTS and rTS. The only other mammalian TS structure so far reported is that for the unliganded human TS at 3.0 Å resolution (*18*). In this structure, none of the mammalian insertions were visible, and the active site cysteine, Cys h195, was found to lie in a nonfunctional conformation with the catalytic thiol buried, possibly due to disulfide bond formation with Cys h180 during purification. In the rTS structures of the present study, two of the three mammalian insertions are visible, and the active site thiol is in the functional position.

DISCUSSION

The two crystal structures of rat TS complexed with dUMP and Tomudex determined in this study provide the first look at a mammalian TS with ligands bound, and provide the first well-resolved models for understanding the structural basis for mammalian-specific TS functions. The most surprising revelation in these structures is that binding of Tomudex to the rat and *E. coli* proteins differs. Rat TS monomers were determined in six different crystalline environments (two in crystal form 1 and four in crystal form 2), and all six were essentially identical and in the "open" conformation. In contrast, the ternary complex formed with *E. coli* TS (*19*) is in the same closed conformation that all ecTS inhibitory complexes have exhibited (*1*). While it is possible that the rTS-dUMP-Tomudex complex may also adopt the closed conformation, it seems clear from the present experiments that the open conformation is the predominant conformer in solution, since it occurs in multiple crystalline environments. No evidence that the observed open conformation was due to artifact was discovered: the protein was determined to be full-length and to have the expected specific activity, and no modifications such as oxidation of sulfhydryls by reducing agent were detected (see, for example, Cys r189 in Figure 2). Further evidence in support of this conclusion comes from kinetic studies: Tomudex inhibition is competitive with CH_2THF for the rat protein, indicating free exchange of both inhibitor and cofactor occurs, whereas inhibitors such as CB3717 (Figure 1) exhibit a slow-binding phase where inhibition changes from competitive to a form with an extremely long off rate (26.5 h for the *L. casei* protein (*45*)). Consistent with the stability of this complex is the ecTS-dUMP-CB3717 structure, which has the closed conformation and a covalent bond between dUMP and Cys ec146 (*12*). Interestingly, rTS complexes with more tightly binding inhibitors such as CB3717 do not crystallize in the same manner as the Tomudex complexes, suggesting that such ligands induce the closed conformation in the protein (Sotelo-Mundo and Montfort, unpublished observations).

The open conformation in the present structures may result from the accumulation of several destabilizing factors. First, the inhibitor has fewer contacts with the protein than other inhibitors such as CB3717. The latter compound can hydrogen bond to the C-terminal loop through its 2-amino group, whereas Tomudex has a 2-methyl in this position. CB3717 also has a bulkier N10 substituent than Tomudex, which makes several contacts with the protein. Second, the rat protein has lost an amino acid contact to the inhibitor through the change of Trp ec83 for Asn r106. Third, the energetic barrier to active site closure may be larger in rTS than in ecTS through the species-specific contacts of Phe r74, which contacts Phe r219 and alters its position such that it now sterically opposes active site closure.

It is interesting that, despite the foregoing discussion, binding of Tomudex to rTS is at least 10-fold tighter than to ecTS. One possible reason for this is that Phe r74 becomes buried on Tomudex binding to rTS, but in ecTS, this residue is a histidine and not involved in binding. A second possible reason is that binding energy is apparently not expended to induce the closed conformation in rTS, whereas in ecTS, some portion of the binding energy must be used to overcome the energetic barrier to closure. A possible design strategy for the improvement of Tomudex would therefore be to further stabilize binding of the inhibitor to the open conformer of rTS. This could be accomplished by, for example, replacing the N10-methyl with a more bulky substituent, or by adding substituents to the quinazoline rings.

ACKNOWLEDGMENT

We thank Dr. Charles Hauer and Dr. Karen Roth of the Wadsworth Center's Mass Spectrometry Core Facility for the rat TS mass determinations, and Dr. Wallace Clark of the University of Arizona Laboratory for Protein Sequencing and Analyses for sequencing the rat TS N-terminus.

REFERENCES

1. Montfort, W. R., and Weichsel, A. (1997) *Pharmacol. Ther. 76*, 29−43.
2. Stroud, R. M., and Finer-Moore, J. S. (1993) *FASEB J. 7*, 671−677.
3. Carreras, C. W., and Santi, D. V. (1995) *Annu. Rev. Biochem. 64*, 721−762.
4. Hardy, L. W. (1995) *Acta Biochim. Pol. 42*, 367−380.
5. Friedkin, M., and Kornberg, A. (1957) in *The Chemical Basis of Heredity* (McElroy, W. D., and Glass, B., Eds.) pp 609−614, The Johns Hopkins Press, Baltimore, MD.
6. Chu, E., and Allegra, C. J. (1996) *BioEssays 18*, 191−198.
7. Samsonoff, W., Reston, J., McKee, M., O'Connor, B., Galivan, J., Maley, G., and Maley, F. (1997) *J. Biol. Chem. 272*, 13281−13285.
8. veer Reddy, G., and Pardee, A. (1983) *Nature 304*, 86−88.
9. Fantz, C. R., Shaw, D., Moore, J. G., and Spencer, H. T. (1998) *Biochem Biophys. Res. Commun. 243*, 6−12.
10. Tong, Y., Liu-Chen, X., Ercikan-Abali, E. A., Capiaux, G. M., Zhao, S. C., Banerjee, D., and Bertino, J. R. (1998) *J. Biol. Chem. 273*, 11611−11618.
11. Hyatt, D. C., Maley, F., and Montfort, W. R. (1997) *Biochemistry 36*, 4585−4594.
12. Montfort, W. R., Perry, K. M., Fauman, E. B., Finer-Moore, J. S., Maley, G. F., Hardy, L., Maley, F., and Stroud, R. M. (1990) *Biochemistry 29*, 6964−6977.
13. Matthews, D. A., Villafranca, J. E., Janson, C. A., Smith, W. W., Welsh, K., and Freer, S. (1990) *J. Mol. Biol. 214*, 937−948.
14. Barrett, J. E., Maltby, D. A., Santi, D. V., and Schultz, P. G. (1998) *J. Am. Chem. Soc. 120*, 449−450.
15. Spencer, H. T., Villafranca, J. E., and Appleman, J. R. (1997) *Biochemistry 36*, 4212−4222.
16. Takemura, Y., and Jackman, A. L. (1997) *Anti-Cancer Drugs 8*, 3−16.

17. Jackman, A. L., and Calvert, A. H. (1995) *Ann. Oncol. 6*, 871−881.
18. Schiffer, C. A., Clifton, I. J., Davisson, V. J., Santi, D. V., and Stroud, R. M. (1995) *Biochemistry 34*, 16279−16287.
19. Rutenber, E., and Stroud, R. (1996) *Structure 4*, 1317−1324.
20. Ciesla, J., Weiner, K., Weiner, R., Reston, J., Maley, G., and Maley, F. (1995) *Biochim. Biophys. Acta 1261*, 233−242.
21. Laemmli, U. K. (1970) *Nature 227*, 680−685.
22. Wahba, A. J., and Friedkin, M. (1962) *J. Biol. Chem. 237*, 3794−3801.
23. Ciesla, J., Golos, B., Dzik, J. M., Pawelczak, K., Kempny, M., Makowski, M., Bretner, M., Kulikowski, T., Machnicka, B., Rzeszotarska, B., and Rode, W. (1995) *Biochim. Biophys. Acta 1249*, 127−36.
24. Rhee, M. S., Balinska, M., Bunni, M., Priest, D. G., Maley, G. F., Maley, F., and Galivan, J. (1990) *Cancer Res. 50*, 3979−3984.
25. Dabrowska, M., Zielinski, Z., Wranicz, M., Michalski, R., Pawelczak, K., and Rode, W. (1996) *Biochem. Biophys. Res. Commun. 228*, 440−445.
26. Otwinowski, Z. (1993) in *Proceedings of the CCP4 Study weekend: Data collection and processing* (Sawyer, L., Isaacs, N., and Bailey, S., Eds.) pp 56−62, SERC Daresbury Laboratory, England.
27. Messerschmidt, A., and Pflugrath, J. W. (1987) *J. Appl. Crystallogr. 20*, 306−315.
28. Kabsch, W. (1988) *J. Appl. Crystallogr. 21*, 916−934.
29. CCP4 (1994) *Acta Crystallogr., Sect. D 50*, 760−763.
30. Fujinaga, M., and Read, R. J. (1987) *J. Appl. Crystallogr. 20*, 517−521.
31. Brunger, A. T. (1990) *Acta Crystallogr., Sect. A 46*, 46−57.
32. Matthews, B. W. (1968) *J. Mol. Biol. 33*, 491.
33. Jones, T. A., Zou, J. Y., Cowan, S. W., and Kjelgard, M. (1991) *Acta Crystallogr., Sect. A 47*, 110−119.
34. Brunger, A. T., Kuriyan, J., and Karplus, M. (1987) *Science 235*, 458−460.
35. Engh, R. A., and Huber, R. (1991) *Acta Crystallogr., Sect. A 47*, 392−400.
36. Kraulis, P. J. (1991) *J. Appl. Crystallogr. 24*, 946−950.
37. Esnouf, R. M. (1997) *J. Mol. Graph. Model 15*, 132−4, 112−3.
38. Ward, W. H. J., Kimbell, R., and Jackman, A. L. (1992) *Biochem. Pharmacol. 43*, 2029−2031.
39. Hardy, L. W., Finer-Moore, J. S., Montfort, W. R., Jones, M. O., Santi, D. V., and Stroud, R. M. (1987) *Science 235*, 448−455.
40. Fauman, E. B., Rutenber, E. E., Maley, G. F., Maley, F., and Stroud, R. M. (1994) *Biochemistry 33*, 1502−1511.
41. Finer-Moore, J. S., Montfort, W. R., and Stroud, R. M. (1990) *Biochemistry 29*, 6977−6986.
42. Finer-Moore, J. S., Maley, G. F., Maley, F., Montfort, W. R., and Stroud, R. M. (1994) *Biochemistry 33*, 15459−15468.
43. Finer-Moore, J. S., Fauman, E. B., Foster, P. G., Perry, K. M., Santi, D. V., and Stroud, R. M. (1993) *J. Mol. Biol. 232*, 1101−1116.
44. Knighton, D. R., Kan, C.-C., Howland, E., Janson, C. A., Hostomska, Z., Welsh, K. M., and Matthews, D. A. (1994) *Nat. Struct. Biol. 1*, 186−194.
45. Pogolotti, A. L., Jr., Danenberg, P. V., and Santi, D. V. (1986) *J. Med. Chem. 29*, 478−482.
46. Hodel, A., Kim, S.-H., and Brunger, A. T. (1992) *Acta Crystallogr., Sect. A 48*, 851−859.
47. Brunger, A. T. (1992) *Nature 355*, 472−475.

BI981881D